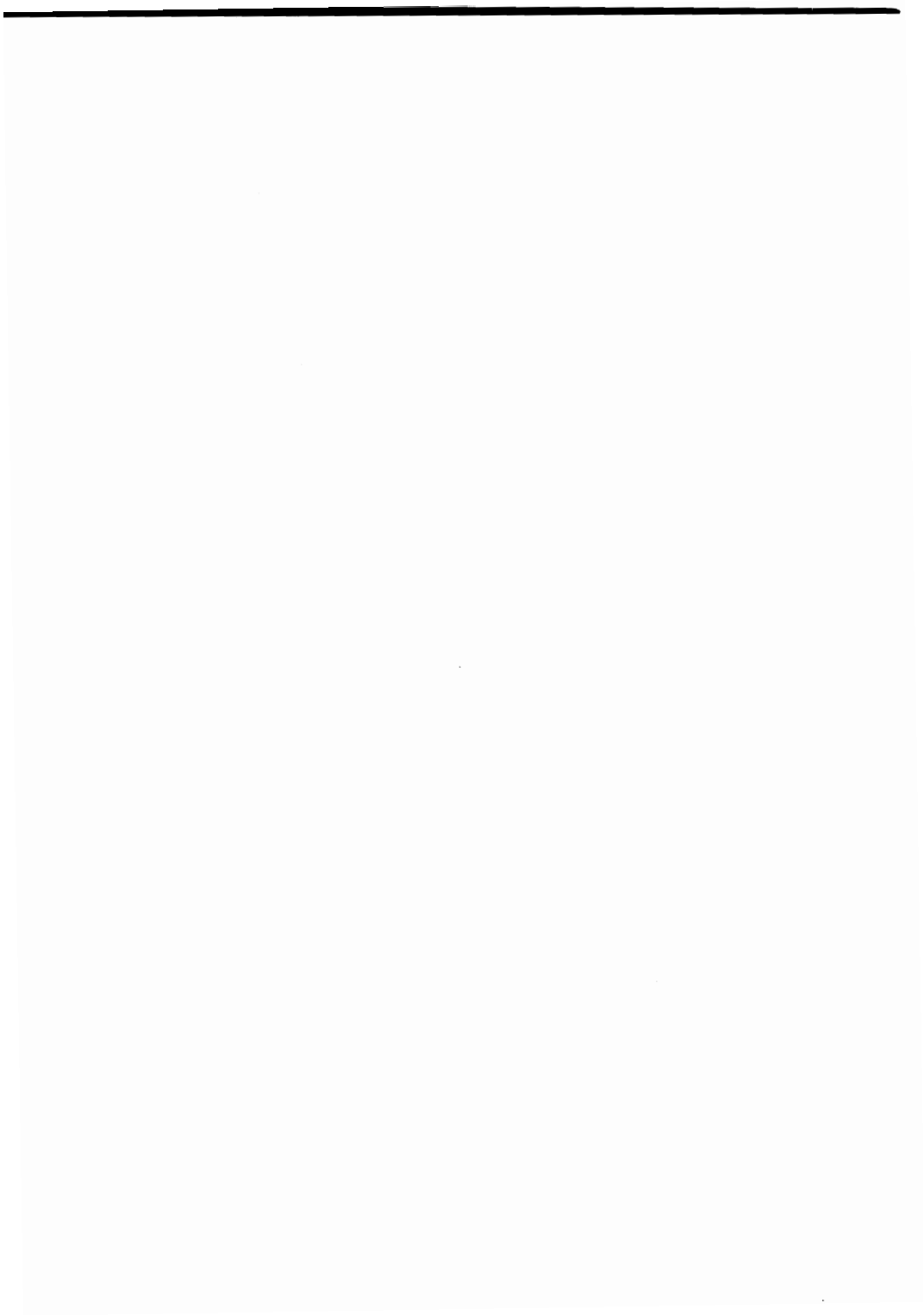


Future Accelerators 

**R. R. Wilson, Fermilab
Session Organizer**



Eberhard Keil
CERN
Geneva, Switzerland

Summary

This paper consists of two parts. The first two chapters are devoted to LEP, the CERN project for an e^+e^- storage ring of about 30 km circumference, covering an energy range from 22 to 130 GeV. The first chapter contains the main considerations upon which the design and the performance estimates are based. The second chapter describes those engineering aspects in which LEP differs most from smaller machines. In the second part, Chapter 3, scaling laws are discussed of several important phenomena for machines even larger than LEP. This includes size and cost, the RF system, interaction region design, beam strahlung, quadrupole radiation, and collective phenomena, e.g. bunch lengthening.

1. LEP Performance

Design concepts¹ for a large electron-positron storage ring (LEP) have been under study at CERN since early 1976. In the first study, 50 km circumference and 100 GeV per beam - to be obtained with a conventional RF system - were chosen. This study² was terminated with several problems still unsolved, including high sensitivity of orbit stability to closed-orbit distortions, operation in collision mode with electrostatically separated beams and technical problems due to the low magnetic field at injection. In addition, the estimated cost was considered high. A fresh start was made in the second half of 1977. In order to explore the variation of difficulties and cost with machine size and in an attempt to arrive at a solid base for an entirely feasible machine, it was decided to reduce the nominal energy to 70 GeV while retaining the target of maximum luminosity at $10^{32} \text{ cm}^{-2} \text{ s}^{-1}$. The optimum radius for this design - later confirmed by the outcome of the study - is 3.5 km. This phase of the study ended in August 1978 with the completion of a detailed Design Report³ including a cost estimate. The conclusions are that such a machine is not only feasible but that it can be developed to reach 100 GeV per beam when suitable superconducting cavities become available. In fact, the design is made such that this extension of energy requires no major change other than the substitution of cavities.

Following strong encouragement by ECFA, the European Committee for Future Accelerators, a somewhat larger machine - LEP Version 8 - has by now been under study for almost a year. A report on this machine, called the Pink Book⁴, has been published. This machine is composed of similar building blocks to those of the previous machine. However, further reductions in cost have been sought by improvements of details and the application of novel solutions to some components.

1.1 Main LEP parameters

The nominal design of LEP includes a maximum luminosity of $10^{32} \text{ cm}^{-2} \text{ s}^{-1}$ at about 86 GeV, to be obtained with copper RF cavities. The design of at least the magnet and vacuum systems permits extension to 130 GeV by means of superconducting RF cavities. The optimum value of the circumference is about 30 km. Its exact value has been chosen so as to permit e-p collisions⁵ in a bypass⁶ to the CERN SPS, respecting the different radio frequencies and bunch numbers in the SPS and LEP. General machine parameters are shown in Table 1.

Table 1. LEP parameters at 86 GeV

Machine circumference		30.6	km
Number of interaction points		8	
Number of bunches		4	
Horizontal tune		70.3	
Vertical tune		74.5	
Length of regular cell		79	m
Beam-beam bremsstrahlung lifetime		8.2	h
Maximum luminosity/ $10^{32} \text{ cm}^{-2} \text{ s}^{-1}$	1	0.5	
Horizontal ampl. fct.	β_x^*	1.6	3.2 m
Vertical ampl. fct.	β_y^*	0.1	0.2 m
Free space	β_x	± 5	± 10 m
Beam-beam tune shift	ΔQ	0.06	0.06

The design of LEP is based on a site near CERN. The machine is almost tangential to the SPS between SPS straight sections 5 and 6 as required for the e-p bypass. The machine is situated underground. The main tunnel will be bored by methods similar to those used for the SPS tunnel and it will have the same width, 4 m. In order not to disturb the landscape outside the immediate vicinity of the eight experimental areas, it is planned to feed the input power, the primary cooling water and all controls connections through the main tunnel.

1.2 Experimental areas

Eight interaction regions are foreseen. Four of them are designed for the nominal luminosity of about $10^{32} \text{ cm}^{-2} \text{ s}^{-1}$ with a free space between the nearest quadrupoles of ± 5 m. Detailed studies⁷ have shown that this is adequate for most foreseeable experiments. In this context, it should be noted that the solenoidal fields which often form a vital part of the experiments can be compensated by skew quadrupoles outside the central region of the insertion. The remaining four interaction regions are designed with a free space of ± 10 m, and have half the nominal luminosity. In the present design, the two types of interaction region alternate around the circumference. Once LEP has been in operation for some time, it might be possible to modify individual interaction regions and to adapt them to the requirements of specific experiments.

Three of the experimental areas are situated in the flank of a mountain range and will be accessible via individual, roughly horizontal access tunnels. The LEP ring will be tilted in such a way that at least two areas come close to, and can be excavated from, the surface. The remaining ones, at most three, will be accessible via vertical shafts. The two latter types of underground experimental area will be very similar to the colliding-beam halls now being constructed for the $p\bar{p}$ project at the SPS.

The size of the experimental hall is determined by the experiments to be performed and the manner in which they are to be installed, operated and eventually changed. The size of the expected experiments is therefore only one of the necessary ingredients. It can be estimated - with considerable uncertainty - from the present generation of experiments at PETRA and PEP. The resulting central detector is roughly a cube with sides 10 m long. Forward detectors for certain experiments, two-photon for example, are expected to extend ± 15 m along the beams.

Table 2
Energy Stages

Stage	1/6	1/3	1	4/3	2
Design energy	49.4	62.3	86.11	92.86	130 GeV
Luminosity	0.385	0.616	1.07	1.15	$1.04 \times 10^{32} \text{ cm}^{-2} \text{ s}^{-1}$
Current	5.71	7.20	9.15	9.15	6.16 mA
RF power	16	32	96	128	96 MW
Length of RF	272	543	1629	2172	1629 m
Number of five-cell room-temperature cavities	128	256	768	1024	-

On the other hand, space requirements for installation and access can be rather safely predicted as they are defined more by the size of the basic components of an experiment which can be conveniently transported and handled.

It is also important that the installation and exchange of experiments in one area does not require long shutdowns of the whole machine. For LEP, where apart from two-photon experiments the detectors are relatively compact, this is most easily provided for by mounting experiments on rails perpendicular to the beam. A rapid exchange can then be carried out if an installed experiment can be rolled out to one side and a previously fully mounted experiment rolled in from the other. This push-pull mode of operation with experiments of the size discussed requires a total hall length transverse to the beams⁷ of about 70 m as shown in Fig. 1.

1.3 Luminosity Variation with Energy

The machine has been designed to reach, with full confidence, an energy at which the best present estimates predict W pair production at a good rate. In its nominal form, called Stage 1, an energy of 86 GeV and a luminosity of $10^{32} \text{ cm}^{-2} \text{ s}^{-1}$ will be obtained by means of an RF system using copper cavities, the only solution which can be safely proposed at present, and an RF power of 96 MW. However, since LEP is expected to be the major European high-energy physics facility in the late 1980s, it must not only offer experimental areas of sufficient size and number, and a high peak luminosity at a nominal energy, but also adequate luminosity over a wide range of lower energies and the potential of extension to considerably higher energies. In our study, particular attention was paid to the last point. Between 22 and 86 GeV, the luminosity is proportional to E^2 . This variation is obtained by a system of wiggler magnets. Once LEP is in operation, the low-energy luminosity might be increased somewhat by filling more of the aperture with beam. With an RF system using copper cavities, the LEP performance at high energies is limited by the RF power dissipation in the cavities. There is good reason to believe, however, that superconducting cavities, whose basic development is being actively pursued in several laboratories, will become operational with adequate performance and at reasonable cost during the lifetime of LEP. Therefore, a Stage 2 using superconducting RF cavities is foreseen for energies much above 86 GeV.

The circulating current is assumed to be limited by collective phenomena at injection and hence kept constant up to an energy where most of the available RF power is converted into synchrotron radiation. Above that energy, about 117 GeV, the synchrotron radiation power is kept constant. The maximum energy at full luminosity, 130 GeV, is determined by the installed RF power. The accelerating gradient in the cavities reaches 5 MV/m at this energy. The magnet and vacuum systems will be constructed so as to permit this extension to 130 GeV with only minor modifications, as soon as a suitable RF system becomes available.

Since, on the other hand, it may seem desirable to start colliding-beam physics at the earliest possible moment, albeit at reduced energy, a staged construction of LEP may be envisaged. The most economic and practical staged construction method consists of installing a fraction of the RF system and the complete magnet and vacuum systems. For the purpose of discussion we have singled out the stage of construction, called Stage 1/3, in which one third of the full complement of cavities and power sources is installed. In Stage 1/3, an energy of 62 GeV with a luminosity of $0.6 \times 10^{32} \text{ cm}^{-2} \text{ s}^{-1}$ can be obtained, making LEP a very worthwhile Z^0 factory. The option is left open of continuing by either installing the full complement of room-temperature cavities to reach Stage 1, or, possibly, going to superconducting cavities at once. Colliding beams of worthwhile energy could still be obtained when only 1/6 of the nominal complement of room-temperature cavities and power sources is installed. Should, against all expectations, superconducting cavities not become available, it would be possible to install an additional 1/3 of the nominal complement of copper cavities in the reserve space foreseen in the lattice, while increasing the RF power to 128 MW. In this Stage 4/3, the maximum energy would be about 93 GeV at full luminosity, and about 100 GeV at 10% luminosity.

The projected luminosity variation with energy in these stages is shown in Fig. 2. A summary of the most important parameters of these stages is given in Table 2.

1.4 The beam-beam limit

The beam-beam limit describes the maximum permissible change in the tune of the machine, i.e. the number of

betatron oscillations in one turn, by the focusing effect of the electromagnetic field due to one bunch on a counter-rotating bunch, for one beam-beam collision, and for particles with betatron amplitudes small compared to the beam size. Since the charge density distribution inside the beam is not uniform, but rather Gaussian, the forces are non-linear. It is their non-linearity which is believed to be at the origin of the beam-beam limit, and the linear beam-beam limit ΔQ is just a convenient measure of the strength of the non-linear forces of the beam-beam interaction. If the forces were linear, the tune-shift would be the same for particles of all amplitudes, and its effects could easily be compensated by a slight retuning of the low- β insertions.

The performance described in the last section is obtained by assuming that the linear beam-beam limit is at $\Delta Q = 0.06$. In this assumption, we follow the practice in the most recent machine designs, PEP⁸, PETRA⁹ and CESR¹⁰. This figure corresponds to the highest values experimentally observed in ADONE¹¹, SPEAR¹² and VEPP-2M¹³. More recent data from DCI¹⁴ and SPEAR¹⁵, and also from PETRA¹⁶, have led to some doubts as to whether a tune shift $\Delta Q = 0.06$ can actually be achieved in LEP. In this context, four questions arise:

- i) What is the beam-beam limit ΔQ ?
- ii) Does it depend on the energy E ?
- iii) Does it depend on the number of bunches k ?
- iv) Does it depend on the exact tune?

The available data have been analysed¹⁷ in terms of a model¹⁸ which essentially calculates the beam blow-up like a diffusion process and compares the blow-up rate to the damping rate from synchrotron radiation. In the existing machines, there are two regimes, which I shall call diffusion regime and stochastic regime, for lack of better names. In the diffusion regime, ΔQ varies like $E^{3/2}$ and like $k^{-1/2}$. In the stochastic regime, ΔQ should be independent of E , but its dependence on k is not known (logically, it should also be independent of k). The diffusion regime is typical for the lower energies in the operating range of a machine like SPEAR. At higher energies the stochastic regime takes over and the tune shift becomes a constant. As the energy and size of the machine increase, the number of beam-beam collisions in a damping time is reduced. Therefore, the energy range of the diffusion regime shrinks, and the energy range of the stochastic regime grows. This should be observed in machines like CESR, PEP and PETRA. The experimental data from these machines are therefore very relevant for the design of LEP which is expected to be almost entirely in the stochastic regime.

From the data already available, a tune shift $\Delta Q = 0.03$ is a safe lower limit. In principle, it would be possible to obtain the same luminosity at half the beam-beam tune shift just by doubling the current. But there are several serious drawbacks in doing this, such as the longer filling time for positrons, stronger collective instabilities in particular at injection, and higher RF power. When discussing the consequences of a smaller value of the beam-beam limit, e.g. $\Delta Q = 0.03$, it is therefore more reasonable to keep the circulating current constant, and hence a reduction in luminosity is inevitable. However, there is sufficient flexibility in the LEP lattice and its aperture is large enough for increasing the beam size as required to keep the luminosity proportional to ΔQ . Hence, the overall result of reducing ΔQ from 0.06 to 0.03 is a loss in luminosity by about a factor of two over the whole energy range. Having established this lower bound for the luminosity, we believe that it would be premature to change the design value of ΔQ at this moment, since this change would have little consequence

on the lattice design.

2. LEP Engineering

This chapter of the LEP description is devoted to engineering aspects in which LEP differs most from other electron-positron storage rings.

2.1 Magnet system

The dipoles are designed as C-magnets. Their lengths are about 6 m for reasons of mechanical rigidity. They will be made of precisely punched steel laminations and concrete¹⁹, the field distribution in the gap being determined by the steel profile. The unusually low field, 0.123 T at 130 GeV, permits a reduction of the steel filling factor to less than 0.3 without leading to saturation. To this end, spacers are pressed into the laminations by the punching die, so that the laminations of 1.55 mm thickness will be spaced at 5.5 mm pitch once they are stacked in a jig. Then the assembly is placed in a mould and the space between laminations is filled with a low shrinkage, corrosion-resistant mortar composed of cement and finegrain silica. Longitudinal tie rods, passing through punched holes near the outer edges of the laminations, will precompress the mortar. As the price of the mortar is very much lower than that of punched laminations the cost of these steel-concrete cores will be substantially reduced - by about a factor of two compared with a conventional core. Other advantages of the steel-concrete cores are their much-improved mechanical rigidity and their reduced weight (also by a factor of two). So far, three models of half cross-sectional scale and 60 cm length have been tested with very encouraging results. A full-size magnet has been completed (Fig. 3).

The low field required also permits excitation by simple aluminium-bar conductors instead of the usual multiturn coils. Several cores can be placed end-to-end with little or no space lost, and excited by one set of bars. A regular half-cell contains six dipoles arranged in this way. All dipoles are connected in series.

The strength of the lattice quadrupoles is entirely governed by 130 GeV operation, requiring an increase in gradient from 4.1 T/m at 86 GeV to at least 10 T/m at 130 GeV. Their cores will be of conventional construction, i.e. they will be made of densely stacked punched laminations. However, the excitation coils will be fabricated from anodized aluminium strip. In Stage 1, all insertion quadrupoles can be of conventional copper-steel construction, but the strongest ones then become rather large, with a length of about 5 m and a diameter of about 1.1 m. It may be advantageous in Stage 1, and it will be necessary in Stage 2 to build the strongest ones as superconducting magnets. A superconducting LEP insertion quadrupole would have half the transverse size of a copper-steel one and present much less interference with the experiments.

2.2 Vacuum system

The linear density of synchrotron radiation hitting the dipole chamber is 1.1 kW/m at 86 GeV and 3.9 kW/m at 130 GeV. These figures are of the same magnitude as those for PEP⁸ or PETRA⁹. The critical energies are 400 keV and 1.4 MeV, respectively. They are about an order of magnitude higher than in PETRA or PEP. This fact and the lower magnetic field in the dipoles pose new problems for LEP although the basic vacuum system design involves a water-cooled chamber made of extruded aluminium and distributed sputter ion pumps immersed in the dipole field, similar to those of SPEAR²⁰, PETRA and PEP.

Considerable thickness of lead shielding is required to prevent an excessive amount of radiation in the tunnel, where corrosive and toxic chemicals would be generated from air and humidity. The lead shield required for Stage 1, 8 mm at the sides of the chamber and 3 mm opposite the magnet poles, will be bonded to the aluminium chamber by a continuous process of melting and extrusion. For Stage 2, additional shielding will be installed between the magnet poles. The high quantum energy occurring in Stage 2 will give rise to noticeable neutron production in the chamber walls and in the cooling water. However, this does not seem to present a serious problem.²¹

The distributed outgassing load due to radiative and thermal desorption will be absorbed by a linear, distributed sputter-ion pump situated in the field of the main dipole magnets. The pole width, determined by requirements of field uniformity, accommodates pump cells of 50 mm diameter. The discharge in these cells can be maintained down to about 180 Gauss, well below the injection field of LEP. Cells of smaller diameter will be inserted to improve the pumping speed at higher fields. Nevertheless, in order to obtain the required low pressure, in situ bakeout (by means of electric heaters attached to the chamber) and in situ glow-discharge (by means of the pump electrodes) are foreseen. In order to arrive at an acceptable cost for the 22 km of distributed pumps the pump anodes will be made of superimposed layers of thin stainless steel strips²² which will be fabricated in a continuous process. Fig. 4 shows a cross-section of the vacuum chamber.

2.3 RF system

At the nominal parameters of Stage 1, $E = 86 \text{ GeV}$ and $L = 10^{32} \text{ cm}^{-2} \text{ s}^{-1}$, the RF system has to make up for 1.37 GeV of energy loss per turn and 25.1 MW of power loss due to synchrotron radiation. With the parameters finally chosen a peak RF voltage of 1.95 GV is required to cover also the parasitic electromagnetic energy losses (110 MeV per turn) and to provide over-voltage for sufficient quantum lifetime.

Following well-established practice, we propose to supply this voltage and power by an accelerating structure consisting of five-cell slot-coupled cavities fed by high-power CW klystrons. There will be 768 cavities fabricated from copper and operating at 353 MHz. They occupy 1630 m of active length, the total length being divided into 16 equal stations, located on either side of all interaction areas. To this conventional system we propose to add a device that decreases the power dissipation in the cavities by a factor 1.5 by modulation. The method consists of coupling a low-loss, H-mode, storage resonator to the accelerating cavity and exciting the coupled system, with CW power sources, at both its resonant frequencies. This makes the stored energy oscillate between the two resonators, spending on average half the time in the low-loss environment. The coupling is adjusted to make peaks of the accelerating field coincide with the passage of a pair of e^+e^- bunches. One common storage resonator is sufficient for each five-cell accelerating cavity. Fig. 5 shows a conceptual design, employing a spherical storage resonators (H_{110} -mode in spherical coordinates) formed from copper sheet. With this system, a total RF generator power of 96 MW enables 86.1 GeV to be reached at full luminosity, about 6 GeV more than the same system would reach without storage cavities.

The frequency of 350 MHz has been chosen in the region of an economic optimum involving effective shunt impedance, fabrication cost of cavities and cost of RF power. The strong longitudinal focusing resulting from this high frequency leads to some beam-dynamical

problems. To alleviate these, a third-harmonic RF system is foreseen.

At the present time klystrons are considered the most advantageous power sources. A power conversion efficiency of 70% has been demonstrated. It is planned to install 96 klystrons - six per RF station - of 1 MW each and to branch out power to the cavities via a chain of hybrid power dividers. Alternative power sources are being studied, however, with the aim of achieving even higher efficiencies or a simplification of power distribution to the cavities.²³

The performance of room-temperature accelerating structures might be further improved by more intense modulation or pulsing. However, only superconducting accelerating cavities will permit the achievement of the full performance potential of LEP. An active development programme is under way and no fundamental limitations known at present appear to preclude accelerating fields four to five times above the values currently used in room-temperature cavities for storage rings. LEP has been designed so that a progressive conversion to RF superconductivity is possible whenever the new technology is ready. We anticipate that superconducting cavities can be economically built for the same frequency as copper cavities so that the power sources can be retained in a conversion. A maximum energy of 130 GeV at $10^{32} \text{ cm}^{-2} \text{ s}^{-1}$ nominal luminosity will be reached when all the Stage 1 RF power is converted to beam power (including parasitic electromagnetic losses). If the superconducting structure achieving this has the same active length, 1630 m, as foreseen for Stage 1, an accelerating field of 5 MV/m will be required.

3. Scaling of e^+e^- Storage Ring Parameters

The following discussion is restricted to comments on how the most important machine parameters and phenomena scale with the design energy in e^+e^- storage rings even larger than LEP. No attempt is made to combine all these scaling laws into one consistent procedure for designing e^+e^- storage rings.

3.1 Size and cost

A design procedure for e^+e^- storage rings²⁴ exists which allows a list of machine parameters to be computed, starting from a relatively small number of assumptions, such as energy E , luminosity L , beam-beam tune shift ΔQ , amplitude function at the crossing point β_y^* , bending radius etc. The relationship between the energy and size of a machine was obtained by Richter²⁵ using cost optimization based on unit prices for tunnels equipped with a FODO lattice, tunnels equipped with RF cavities made of copper and operated CW, RF power installations, and electricity cost. Similar procedures were developed by Ritson²⁶ for pulsed RF systems and Bauer²⁷ for superconducting ones.

The result of Richter's cost optimization is that the size of a machine, and hence its cost, scales approximately like the square of the energy. The scaling laws for other quantities given below will be based on the assumption that the size scales like E^2 exactly. This result can be made plausible by the following two observations.

In the design of the RF system a balance must be found between the cost of the cavities which is proportional to their length L_c , and the cost of the RF power which is proportional to $1/L_c$ when the RF power delivered to the beam is ignored. It is intuitively obvious that the balance is obtained at a given voltage gradient, independent of the machine energy. The optimum gradient is quite low, about 1 MV/m, far below

the breakdown limit of copper cavities. The cavity length is proportional to the synchrotron radiation loss, $L_C \sim U_S$ if the variation of the stable phase angle with energy and the higher-mode voltage U_{hm} are neglected.

In the design of the whole machine an optimum must be found between for the total cost of the whole RF system and the cost of the bending arcs. Here it is intuitively obvious that this optimum is reached when the fraction of the machine circumference occupied by the RF system is independent of the energy, i.e. when the machines are similar, and ρ and L_C scale in the same manner, as long as the unit prices are independent of the energy. Since the synchrotron radiation loss $U_S \sim E^4/\rho$, the product ρL_C scales like E^4 , and ρ and L_C scale like E^2 . The number of stored particles N is related to the luminosity L and the machine parameters by the following equation:

$$L = \frac{N f \gamma \Delta Q}{2 r_e \beta_y^*} \quad (1)$$

where f is the revolution frequency, r_e the classical electron radius, and γ the relativistic factor, and β_y^* the vertical amplitude function at the crossing points.

3.2 RF system

The total RF power which has to be supplied by the power sources is made up of several contributions, the dissipated power in the cavities P_d , the synchrotron radiation power P_b , the higher-mode power P_{hm} , and the reflected power due to the transient beam loading. The largest fraction is the dissipated power P_d which scales like E^2 . The synchrotron radiation power P_b scales like $E L \beta_y^* / \Delta Q$.

Since P_b scales with a lower power of E than P_d , the fraction of the total RF power transferred into the beam decreases with energy if the other parameters remain the same. This is a good reason to look for alternatives to copper cavities driven by CW power sources. Two alternatives have been proposed. Pulsing the power sources might become attractive when the time between bunches becomes long compared to the RF filling time. Superconducting RF cavities would reduce the dissipation by a large factor.

The higher-mode losses are due to the excitation of electro-magnetic fields in the cavities by the passage of the short intense bunches. They have two effects on the RF power requirements. The power P_{hm} corresponding to them has to be supplied to the beams. At a given frequency and bunch length it scales like $(L \beta_y^* E / \Delta Q)^2 / k$, but is usually negligible. The second effect is the additional dissipated power because the cavity voltage has to be increased to compensate the higher-mode voltage U_{hm} . At a given frequency and bunch length $U_{hm} \sim E^3 L \beta_y^* / (k \Delta Q)$. As long as $U_{hm} \ll U_S$, the dominant term in the additional dissipation scales like $E^3 L \beta_y^* / (k \Delta Q)$, i.e. more steeply than P_d .

With a constant RF voltage gradient the stored energy per unit length in the cavities depends only on the RF frequency. On the other hand, the energy which has to be supplied to the beam, per unit length, in a single passage through the cavities, is proportional to N/k . Hence the ratio between extracted and stored energy scales like $E L \beta_y^* / \Delta Q k$. The consequences of all these observations cannot be expressed as a simple power law in a few variables. However, the standard transient beam-loading calculation²⁸ automatically takes care of them; the result for a sample of machines is shown in Fig. 6. It is scaled from LEP-70, and assumes constant L , β_y^* , k and Q and no storage

cavities. The lowest curve just gives the sum $P_b + P_d$ when the higher-mode losses vanish, the second curve includes the transient beam loading, the third curve includes the higher-mode losses but not the transient beam loading; the top curve includes everything. It is clear that the most simple-minded approach, the bottom curve, can lead to considerable underestimates in the total RF power.

So far, it has been tacitly assumed that the frequency was about constant in the scaling operation. It was largely chosen bearing in mind the availability of high-power RF sources and the cost of RF cavities. However, there are several phenomena which favour a lower frequency. One of them is synchro-betatron resonances which can occur when the betatron tune Q and the synchrotron tune Q_s of a machine are related by

$$Q \pm n Q_s = p \quad (2)$$

where n and p are positive integers. In machines like SPEAR²⁹ and PETRA³⁰, with $Q_s \approx 0.05$ synchro-betatron resonances are a nuisance because crossing them is associated with beam loss. In order to avoid this the working point Q has to be chosen carefully and controlled very well. In LEP, $Q_s = 0.16$, unless it is reduced by a third-harmonic RF system. It is easy to relate Q_s to the performance parameters of the machine:

$$Q_s \geq \left(\frac{2 r_e}{c} \right) \left(\frac{4 \pi^3 r_e c}{27 C_q^2} \right)^{1/6} (-f_{RF} R \cot \phi_s)^{1/2} \times \left(\frac{\gamma}{\rho} \right)^{1/6} \left(\frac{\beta_y^* L}{k \Delta Q^2} \right)^{1/3} \quad (3)$$

Here, c is the velocity of light, $C_q = 3.84 \times 10^{-13} m$, and ϕ_s is the stable phase angle. The equals sign applies when higher-mode losses are neglected. It follows that for constant Q_s , f_{RF} has to scale as follows:

$$f_{RF} \sim E^{-5/3} (k \Delta Q^2 / \beta_y^* L)^{2/3} \quad (4)$$

In order to keep Q_s constant the frequency has to scale like $E^{-5/3}$ at constant k ; or k has to be increased like $E^{5/2}$ at constant f_{RF} . In the latter case the bunch spacing decreases because k increases faster than the machine size.

Pulsed travelling-wave RF systems look most attractive when the frequency and the bunch spacing are high.³¹ This requirement conflicts with the above condition for constant Q_s .

3.3 Interaction region design

In order to obtain the desired luminosity with the minimum circulating current, the design of e^+e^- storage rings nowadays includes low- β insertions. In this way, the beam size at the interaction point is made particularly small. This has several consequences which will be discussed in this section.

The consequences of optical limitations on the design of the interaction regions³² can be qualitatively discussed in the following way. The rms beam size at the crossing point is known. In thin-lens approximation it can be extrapolated to the centre of the nearest quadrupole which is at a distance ℓ_x from the crossing point. Constraints on ℓ_x due to the size of experiments are ignored for the time being. The aperture of this quadrupole must be a factor $F_a \approx 10$ larger

than the rms beam size in it. The quadrupole field at the edge of the aperture B_Q is determined by its construction technique, $B_Q \approx 1$ T for a copper-steel quadrupole and higher for a superconducting one. In order to obtain the focal length imposed by the optics, which is roughly $\frac{1}{2} \ell_x$, the physical quadrupole must have a length ℓ_Q . Optics prohibits too small ratios $G_\ell = \ell_x / \ell_Q$, we use $G_\ell \approx 1.5$. Finally, the chromatic effects of the quadrupole must be considered. Since they must be corrected for a momentum bite of about $\pm 1\%$, the ratio $G_c = \ell_x / \beta_y^*$ cannot be larger than 50 to 100. Applying all these considerations yields a formula for β_y^* :

$$\beta_y^* = \frac{G_\ell F a}{G_c} \frac{e Z_0}{2\pi B_Q \Delta Q} \left(\frac{L \beta_y^*}{\pi k f \beta_x^*} \right)^{1/2} \quad (5)$$

Here $Z_0 = 120 \pi \Omega$ is the impedance of free space. On the right-hand side only the ratio β_y^* / β_x^* appears. If the aperture calculation had been done for full coupling, this factor would have dropped out. Applying equ. (5) to the high-luminosity LEP insertion gives good agreement. Equ. (5) implies that $\beta_y^* \sim E$ if all other terms are kept constant. Constant β_y^* could be achieved by having $k \sim E^2$, a less steep variation than that required by the synchrotron tune Q_s (Section 3.2).

Two other phenomena entering into the design of the interaction regions are related to synchrotron radiation. Any electron which is deflected with a bending radius ρ emits synchrotron radiation corresponding to an energy loss per unit length given by

$$\frac{dU}{ds} = - \frac{2}{3} \frac{r_e E_0 \gamma^4}{e \rho^2} \quad (6)$$

Here E_0 is the electron rest energy. This also holds for particles which pass a quadrupole field off-axis. This happens in two places in an interaction region, in the field of the opposite beam, and in the quadrupole magnets. Since the bending radius in a quadrupole is proportional to the distance from the axis, these phenomena depend on the particle amplitude. Here they are calculated for one standard deviation.

The first phenomenon³³ was dubbed "beam strahlung". In this case the bending radius is relatively small, some 200 m in LEP, and the interaction length is comparable to the bunch length σ_z . This implies that the critical photon energy is high and the number of photons emitted by one particle in a collision is low. Therefore the dominant effect of beam strahlung is a contribution to the energy spread of the beam. If the condition is imposed that this contribution be no larger than the energy spread in the absence of beam strahlung, the following relation must be satisfied:

$$L^{3/2} E^4 n_x / \sigma_z^2 k^{3/2} \leq 10^{66} \quad (7)$$

Here n_x is the number of crossing points. Distances are measured in metres, the energy in GeV, and $10^{32} \text{cm}^{-2} \text{s}^{-1} = 10^{36} \text{m}^{-2} \text{s}^{-1}$. Equ. (7) is independent of the beam-beam limit ΔQ , but assumes as in LEP that the ratio of the beam sizes at the crossing points is $\sigma_y^* / \sigma_x^* = 0.06$. For parameters similar to those of LEP, $L = 10^{32} \text{cm}^{-2} \text{s}^{-1}$, $n_x = 8$, $k = 4$, $\sigma_z = 0.063$ m we find $E < 250$ GeV. This limit is probably pessimistic because of the approximations used in calculating the curvature. If beam strahlung is not to be a problem at higher energies, the bunch length σ_z and/or the bunch number k must be increased.

The quadrupole radiation as it shall be called here is mainly generated in the insertion quadrupoles.

Its characteristics differ from that of the beam strahlung. The bending radius and hence the critical photon energy are more comparable to those in the dipoles. In addition the length of the quadrupole is much higher than the bunch length and hence the number of photons emitted by one particle when passing the quadrupole is higher. Therefore the dominant effect of quadrupole radiation is its contribution to the energy loss, while its contribution to the energy spread is negligible.

By arguing about the quadrupole aperture and strength in the same way as above one can obtain an expression for the ratio of the synchrotron radiation losses in an interaction region quadrupole U_Q to those in the bending arcs U_s :

$$U_Q / U_s = \left(\frac{r_e c e}{\pi E_0} \right) \frac{B_Q \rho}{F_a \gamma^2 \Delta Q} \left(\frac{L}{2\pi f k} \right)^{1/2} \quad (8)$$

The stable phase angle now becomes a function of the betatron amplitude³⁴. Other consequences of quadrupole radiation are being studied³⁵. With all parameters except f fixed and with $f \sim E^{-2}$, $U_Q / U_s \sim E$. If $k \sim E^2$, the ratio U_Q / U_s becomes a constant.

Both beamstrahlung and quadrupole radiation are potential sources of background for experiments installed in the interaction regions.

3.4 Bunch lengthening

Bunch lengthening and widening is observed in all operating e^+e^- storage rings. As suggested by the names, the length and the energy spread of the bunches for finite current I are larger than for vanishing current. The reason for this is believed to be a turbulent instability³⁶, driven by the impedance which the vacuum chamber and the RF system present to the beam. The same impedance also causes the higher-mode losses discussed in Section 3.2.

The energy spread σ_e due to the turbulent instability is given by

$$\sigma_e^3 = \frac{Q_s^3}{\alpha^3} \frac{(2\pi)^{1/2} I}{k h V_{RF}} \left| \frac{Z/n}{\cos \phi_s} \right| \quad (9)$$

Here α is the momentum compaction, h is the harmonic number, V_{RF} is the peak voltage of the RF system and Z/n is the impedance, taken at a frequency of about 1 GHz divided by the mode number n , the ratio between 1 GHz and the revolution frequency.

In a modern machine with a rather smooth vacuum chamber, Z/n is dominated by the contribution of the RF system and typically amounts to a few Ω . Bunch lengthening occurs when the energy spread given by (9) exceeds the natural energy spread σ_{eo} due to quantum excitation and radiation damping.

$$\sigma_{eo}^2 = \frac{C_q \gamma^2}{\rho J_s} \quad (10)$$

where $J_s \approx 2$ is the damping partition number for synchrotron oscillations.

If one observes that the quantities occurring in (9) are related to performance parameters such as L , β_y^* and ΔQ , and if one assumes that the machine parameters are adjusted accordingly, one finds for the bunch lengthening $B = \sigma_e / \sigma_{eo}$:

$$B^3 = \frac{e^2 c}{E_0} \frac{\Delta Q |z/n|}{J_x} \left(\frac{\gamma h \cot \phi_s}{3\pi r_e C_q} \right)^{1/2} \left(\frac{J_s C}{2\pi R} \right)^{3/2} \quad (11)$$

Here J_x is the radial damping partition number and R is the average radius of the arcs. The surprising feature of (11) is the absence of parameters such as L , β_y^* , or k .

The significant parameters for B are ΔQ , γ and h . Since $h \sim E^2 f_{RF}$ we conclude that in order to keep B constant when the energy of a machine increases, the RF frequency f_{RF} has to be decreased like E^{-3} . For a given energy, a machine with a superconducting RF system has about half the radius of a machine with a conventional CW RF system.²⁷ Hence, for equal bunch lengthening B and energy E , the radio frequency f_{RF} can be a factor of two higher in a superconducting machine. For equal B and f_{RF} , the energy E in a superconducting machine can be higher by a factor $2^{1/3} \approx 1.26$.

3.5 Conclusions

In order to find our way through the constraints on the machine design imposed by the various phenomena discussed above, we want to express them in terms of the smallest possible set of parameters. For simplicity we assume that L and ΔQ are kept constant. Furthermore, we relate the bunch length σ_z in (7) to the other machine parameters and find that:

$$\sigma_z \sim \left(\frac{\beta_y^* L}{k} \right)^{1/3} \gamma^{-1/6} f_{RF}^{-1/2} (\Delta Q)^{-2/3} \quad (12)$$

We can then express all the scaling laws in terms of only four parameters: E , f_{RF} , k , β_y^* , as shown in Table 3.

Table 3. Summary of scaling laws

No.	Constant	Requires
1	Bunch lengthening	$f_{RF} \sim E^{-3}$
2	Quadrupole radiation	$k \sim E^2$
3	β_y^*	$k \sim E^2$
4	Q_s	$f_{RF} (\beta_y^*/k)^{2/3} \sim E^{-5/3}$
5	Beam strahlung	$f_{RF} k^{-5/6} \sim E^{-13/3}$

The first constraint, due to bunch lengthening, imposes a condition on the radio frequency f_{RF} . As the frequency decreases, the cost of the RF cavities and of the power sources increases rapidly. If we assume that a practical lower limit is $f_{RF} = 50$ MHz and if we are willing to tolerate the same bunch lengthening as in LEP, we find a maximum design energy of $E = 165$ GeV for a copper RF system, or $E = 210$ GeV for a superconducting RF system at the same frequency. For $f_{RF} = 100$ MHz, the corresponding energies are 130 GeV and 165 GeV, respectively.

The second and third constraints relate the number of bunches to the energy. They imply that the bunch spacing must be constant. It follows that the e^+ and e^- beams must be separated by electrostatic plates if they circulate in a single magnet lattice, or that they must circulate in two different magnet lattices. In either case, they must be made to collide with tight

tolerances at the crossing points. This conclusion was already reached in ref. 33 for different reasons. Only a detailed study can show which of the schemes is less unattractive in terms of cost and operational complications. Both of them deviate drastically from present schemes with $k = n_x/2$ in which the collisions between e^+ and e^- bunches are ensured by the CPT theorem.

The last two constraints are automatically satisfied if the above conditions on f_{RF} and k are fulfilled.

Following the above recommendations - decrease f_{RF} like E^{-3} and increase k like E^2 - ensures that none of the phenomena discussed gets worse with increasing energy than in the machine used as a starting point for the scaling. However, these recommendations are sufficiently unattractive, both economically and operationally, that a more detailed study of the limits imposed by all these phenomena would be in order.

Acknowledgements

The LEP description sums up the work of a Study Group based at CERN with wide outside-CERN participation. A list of contributors is given in the Pink Book.⁴

References

1. R. Billinge et al., IEEE Trans. Nucl. Sci. **NS-24**, No.3, pp. 1857-1859 (1977).
2. J.R.J. Bennett et al., CERN 77-14 (1977).
3. The LEP Study Group, CERN Int. rep. ISR-LEP/78-17 (1978).
4. The LEP Study Group, CERN Int. rep. ISR-LEP/79-33 (1979).
5. A. Hutton, IEEE Trans. Nucl. Sci. **NS-26**, 3520 (1979).
6. Y. Baconnier and W. Scandale, CERN Int. rep. SPS/AOP/DV/Note/78-23 (1978).
7. Proc. LEP Summer Study, CERN 79-01 (1979).
8. PEP Proposal, LBL-2688/SLAC-171 (1974). PEP Conceptual Design Report, LBL-4288/SLAC-189 (1976).
9. PETRA Proposal (DESY, Hamburg, 1974). Updated version of the PETRA proposal (DESY, Hamburg) 1976.
10. B.D. McDaniel, Electron-Positron Colliding Beam Facility at Cornell, Cornell Univ. (1975).
11. F. Amman et al., Proc. 8th Internat. Conf. on High Energy Accelerators, Geneva, 1971 (CERN, Geneva 1971), p. 132.
12. SPEAR Group, IEEE Trans. Nucl. Sci. **NS-20** (1973) 838.
13. I.B. Vasserman et al., Proc. 5th All-Union Conf. on Particle Accelerators, Dubna, 1976 (Izdatelstvo Nauka, Moscow, 1977), Vol. 1, p. 252 (in Russian), Eng. trans. as SLAC TRANS-177 (1977).
14. The Orsay Storage Ring Group, LAL/RT/79-01 (1979).
15. M. Cornacchia, PEP Note 275 (1978).
16. A. Piwinski, IEEE Trans. Nucl. Sci. **NS-26**, 4268 (1979).
17. E. Keil, CERN Int. rep. ISR-TH/79-32 (1979).
18. S.A. Kheifets, IEEE Trans. Nucl. Sci. **NS-26**, 3615 (1979).
19. J.-P. Gourber and L. Resegotti, IEEE Trans. Nucl. Sci. **NS-26**, 3185 (1979).
20. U. Cummings et al., SLAC-PUB 797 (1970).
21. W.R. Nelson and J.W.N. Tuyn, CERN Int. Rep. HS-RP/037 (1979).
22. J.-M. Laurent and O. Gröbner, IEEE Trans. Nucl. Sci. **NS-26**, 3997 (1979).
23. C. Zettler, CERN Int. rep. SPS/ARF/79-12 (1979).
24. J.R. Rees and B. Richter, SPEAR-167 (1973).
25. B. Richter, Nucl. Instrum. Methods, **136**, 47 (1976).

26. D. Ritson, PEP Note 280 (1979).
27. W. Bauer, in CERN 79-01, 351 (1979).
28. P.B. Wilson, Proc. 9th Internat. Conf. on High Energy Accelerators, Stanford, 1974 (CONF 740522, USAEC, Washington, 1974) 57.
29. SPEAR Group, IEEE Trans. Nucl. Sci. NS-24, 1863 (1977).
30. G.A. Voss, private communication.
31. P.B. Wilson, IEEE Trans. Nucl. Sci. NS-26, 3255 (1979).
32. E.D. Courant and E. Keil, Proc. Workshop on Possibilities and Limitations of Accelerators and Detectors, Fermilab October 1978, 135 (1979).
33. J.-E. Augustin et al., *ibid*, 87.
34. A.W. Chao and A.A. Garren, PEP Technical Memo 141 (1978).
35. M. Bassetti, private communication.
36. D. Boussard, CERN Report Lab. II/RF/Int./75-2 (1975).

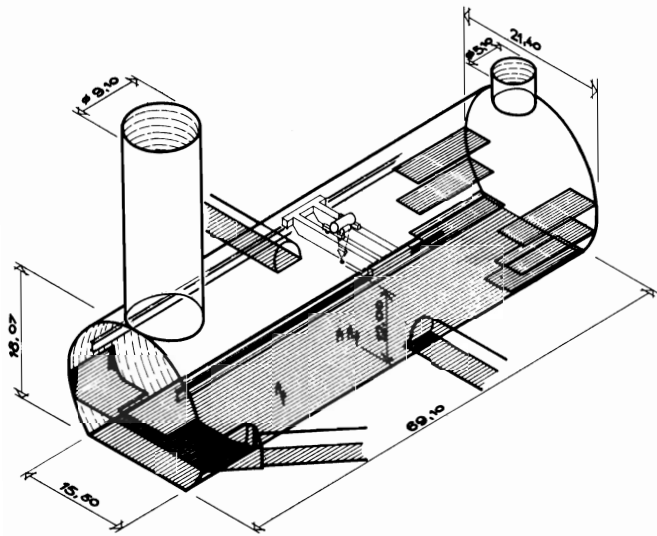


Fig. 1. Schematic view of underground experimental area

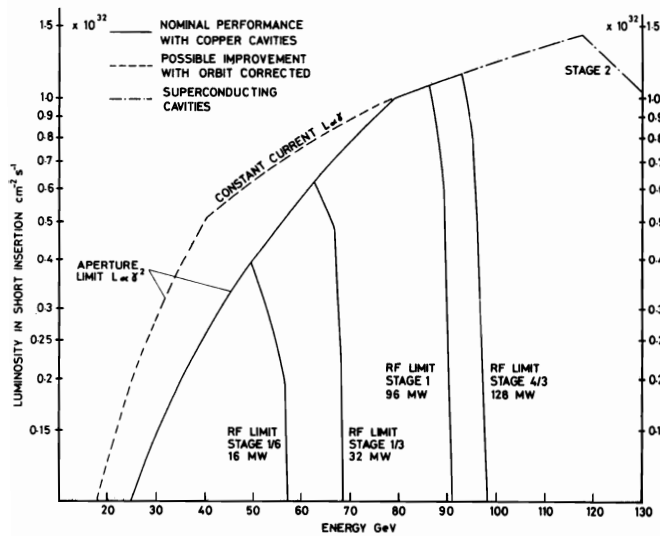


Fig. 2. Projected luminosity variation with energy. The rising curve is determined by the aperture and the circulating current, the falling curves by the RF power. The stages 1/6 to 4/3 refer to the fraction of the copper RF cavities and klystrons installed. In Stage 2, superconducting RF cavities are used.

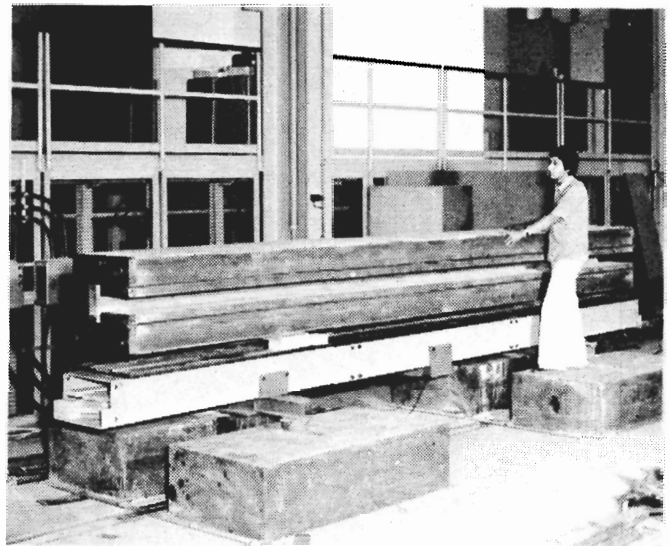


Fig. 3. Full-size prototype of a steel-concrete magnet.

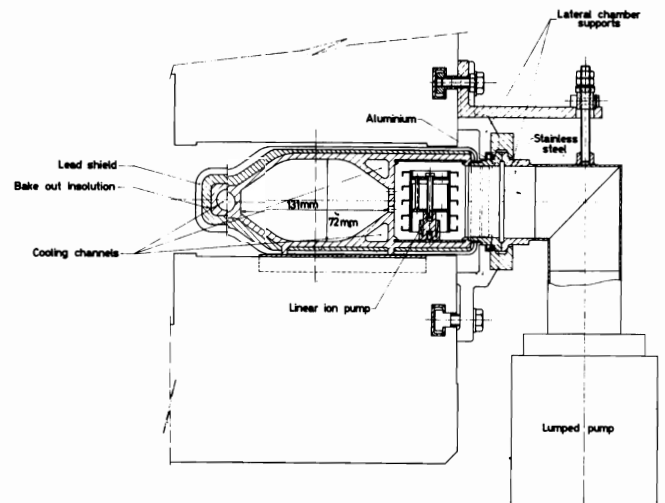


Fig. 4. Vacuum chamber cross-section for dipole magnets showing the arrangement of cooling channels, the chamber supports, the integrated ion pump, and a typical connection for a lumped pump.

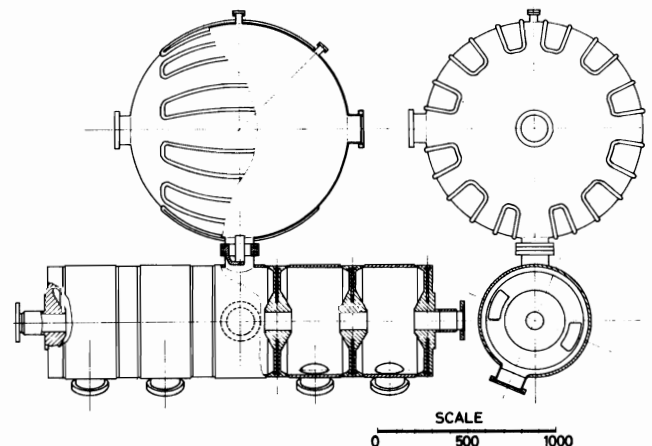


Fig. 5. RF cavity with spherical storage cavity (scale in millimetres)

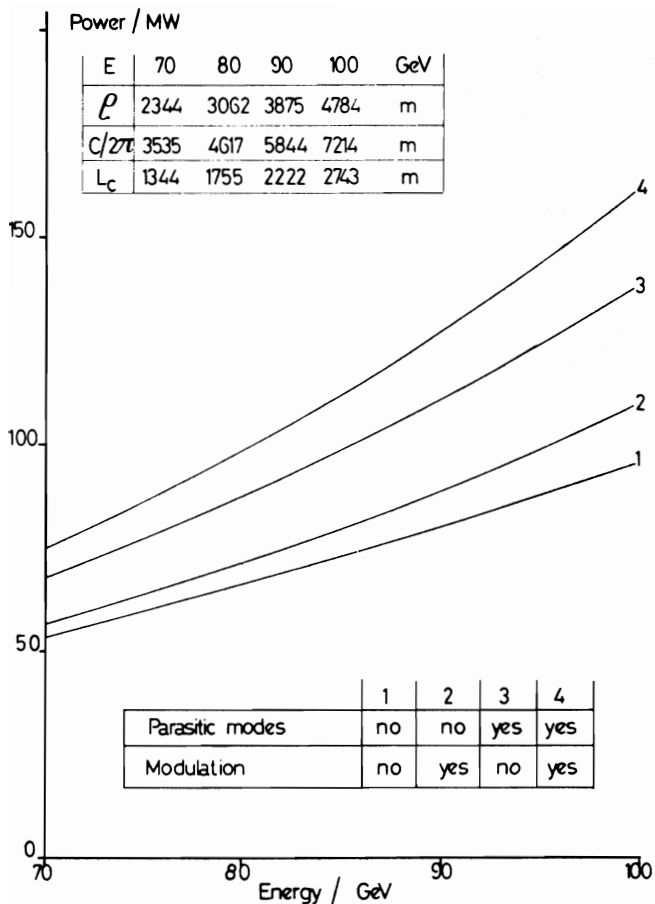


Fig. 6. RF generator power vs. design energy.

Questions and answers

Q. (Gittelman, Cornell) When you speak of a luminosity of $10^{32} \text{ cm}^{-2}\text{s}^{-1}$ do you mean per interaction region?

A. Yes.

Q. (Newman, DESY) Over this enormous machine lattice how big a tolerance is there in the relative machine alignment and given a typical element alignment of, say, 1 mm between magnets, what kind of dispersive forces arise and how does the luminosity change?

A. The tolerance for the magnet position which we worked with is typically 0.1 mm and that has been realized in the SPS. With that alignment tolerance the beam will not circulate in the machine when the low beta insertions are tuned to low beta. Therefore we envisage the possibility, and have made sure that it actually exists, of running the machine with the beta values at the crossing point increased by a factor of 3 in which case even without correction there is a good chance of getting the beam circulating. Once one has a circulating beam one can apply closed orbit corrections and once one has corrected the orbit one can go down to the nominal values of beta. This has all been simulated on computer and looks reasonable.

Q. (Newman, DESY) Are there any non-linear effects involved? For example, at PETRA do you foresee any of these effects being non-correctable or can you suffer misalignments which at the same time don't prevent the beam from circulating but are still somehow not linearly correctable?

A. I think the simulation which we do includes all the effects that are known from PETRA and from theoretical studies.

Q. (Diebold, Argonne) How about scaling the other direction? What could you do with a ring of say a radius of 1 km, such as already exists at CERN and FERMILAB?

A. I think scaling in the other direction makes machines much easier, and I think the scaling laws also apply going in the other direction. The radius will be proportional to the energy squared, so a smaller machine will have a lower energy. I made a small study several years ago of a machine which had 1.1 km average radius because that fitted into the SPS tunnel. And that machine had 40 GeV with conventional copper cavities.

Q. Would that be difficult to boost it up to 45 or 50 GeV to get a Z^0 factory, for example?

A. I think that would not be particularly difficult.

Q. (W. Paul, Univ. of Bonn) Are there any ideas around to make use of this synchrotron radiation power you are wasting?

A. Well, we tell everybody that there is the synchrotron radiation but so far we have not seen anybody who comes running up to us and says he wants to use it. If you can find somebody please let us know.

Q. (Schopper, DESY) I can partly answer it. One idea is that you have a very high entropy in that radiation. Therefore, it's a pity to use it just to warm up water. The only way I could think of using that entropy is in chemical reactions. So we got in contact with some chemists and they are thinking hard about this possibility. They are, for instance, studying its use for polymerization.